

Correlated electrons in a Crystalline Topological insulator

F. Manghi^{1,2}

¹*Dipartimento di Scienze Fisiche, Informatiche e Matematiche,
Università di Modena e Reggio Emilia, Via Campi 213/A, I-41125 Modena, Italy*

²*CNR - Institute of NanoSciences - S3*

(Dated: December 19, 2021)

We study the effects of e-e interaction in a 3D Crystalline Topological Insulator by adding on-site repulsion to the single-particle Hamiltonian and solving the many-body problem within Cluster Perturbation Theory. The goal is to clarify how many body effects modify the topological phase that stems from the crystal symmetries. Tuning the strength of the on-site interaction we show that band inversion disappears in the bulk and surface states loose their metallic character.

PACS numbers: 71.10.-w, 71.10.Fd, 73.20.-r, 73.43.-f

Crystalline Topological Insulators (CTIs) are a new entry in the fascinating class of topological materials. In these systems, the basic ingredients that give rise to topological insulators - time-reversal invariance and spin-orbit interaction - are substituted by crystal symmetries. After the pioneering work that introduced the very notion of CTIs¹, real materials that exhibit this behaviour have been predicted by theory² and revealed by experiments.³⁻⁸ Most of the theoretical studies for both real and model CTIs⁹ have been based on a single particle description of the electronic states and this in spite of the prediction of CTI behavior also for materials where strong e-e correlations are expected.^{10,11} Few works have addressed the effects of electron interactions in CTIs investigating how electron correlations affect their topological classifications¹² or give rise to new topological crystalline Mott insulator phases.¹³ The combination of topological band structure and e-e interactions has been extensively studied in *standard* topological insulators (see Refs. 14–16 for recent reviews). In this field, the two-dimensional honeycomb lattice with intrinsic spin-orbit interaction and on-site e-e repulsion - the so-called Kane-Mele-Hubbard model¹⁷ - has been identified as a paradigmatic example. For this system different many-body approaches have been applied, from Quantum Montecarlo simulations¹⁸⁻²⁰ to Quantum Cluster methods,²¹⁻²³ showing that the Hubbard interaction may drastically affect the stability of the quantum spin Hall phase and suppress topological protected edge states.

In this paper we study the effects of Hubbard correlations on a CTI focusing on quasi-particle states for both bulk and surface systems. We rely our analysis on a solution of the many-body Hamiltonian by Cluster Perturbation Theory (CPT),^{24,25} calculating one-particle propagator and spectral functions. We investigate the effects of e-e interaction in the prototypical CTI introduced by Fu¹ where a tetragonal unit cell hosts two inequivalent atoms with two orbitals per site. This simplified structure, containing different sites and different orbitals, may exhibit non-trivial orbital textures that have been shown to be essential in real CTIs.^{8,26-28} We will see that the many-body effects may drastically modify the band orbital order and consequently affect the CTI phase.

This paper is organized as follows: After a reminder of the single particle properties and an outline of the method adopted to solve the many-body Hamiltonian, the results are shown for both the 3D crystal and the surface-terminated one, illustrating the effects of e-e correlations in terms of orbital order in 3D and of metallic/non-metallic surface states.

Single particle band structure. As mentioned above, the model consists of a tetragonal lattice with two atoms, A and B, per cell and two orbitals per site. Intralayer first- and second- nearest neighbours hopping parameters connect atoms of the same species with values $t_1^A = -t_1^B = 1$, $t_2^A = -t_2^B = 0.5$; intralayer hopping parameters connect sites A and B with values $t'_1 = 2.5$, $t'_2 = 0.5$, $t'_z = 2$ (see (Fig. 1 (a))). An orbital dependence is introduced in the intralayer hopping parameters making them different from zero only when connecting identical orbitals.

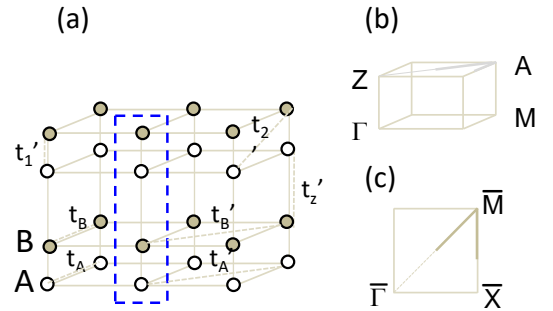


FIG. 1. (a) Tetragonal lattice containing two atomic species. Dashed lines enclose the 4-site non-primitive unit cell that will be used as the cluster for CPT implementation (see next section). (b) 3D Brillouin Zone and high symmetry points. (c) 2D Brillouin Zone and high symmetry points.

The 3D crystal is insulating and this thanks to the hopping between sites A and B: indeed, neglecting them, one would get the band structure reported in panel (a) of Fig. 2 where bands localized on A sites intersect the corresponding bands associated to B sites. The inclu-

sion of interlayer hopping opens the gap and gives rise to the peculiar orbital texture where states of predominant A and B character interchange along the valence and conduction band edges (panel (b) of Fig. 2). The site composition gives rise to a particular mechanism of *band inversion* essential for the occurrence of topologically protected metallic surface states. Indeed band inversion is ubiquitous in topological materials: it can be associated to orbital and/or spin degrees of freedom^{29–33} or to atomic composition^{4,8}. The evolution of band inversion with e-e interaction will be the main result of this paper.

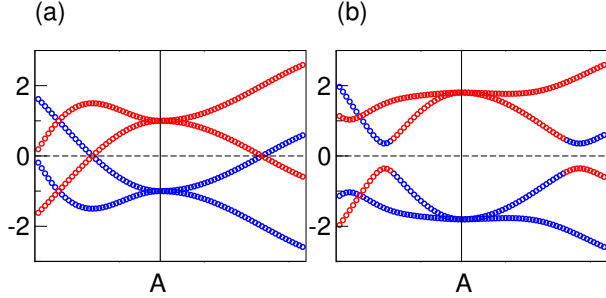


FIG. 2. (a) Single-particle band structure calculated at k-points around A where the minimum energy separation between valence and conduction band occurs. In blue (red) eigenvalues of predominant A- (B) character. Panel (a) reports eigenvalues obtained with no intralayer hoppings ($t'_1 = t'_2 = t'_z = 0$); panel (b) eigenvalues obtained with hopping parameters of ref. 1.

In order to study the reduced dimensionality we have adopted a slab geometry by stacking 20 A-B bilayers along the (001) axis; in this configuration we have both A- and B-terminated surfaces and correspondingly surface states localized either on A or B sites (Fig. 3 (b)). The same slab geometry can be used as a non primitive unit cell to calculate bulk states, getting the so-called Projected Bulk Band Structure (PBBS) (Fig. 3 (a)). As currently done in surface physics³⁴ PBBS allows to identify straightaway the energy regions that, prohibited in the bulk, can host localized states at the surface. The orbital texture of PBBS whereby the A and B bands alternate across the gap edges is also shown.

Interacting Crystalline Topological Insulator
The interacting Hamiltonian reads:

$$\hat{H} = \sum_{\alpha\beta} \sum_{ijll'} t_{il\alpha,jl\beta} \hat{c}_{il\alpha}^\dagger \hat{c}_{jl'\beta} + U \sum_{i\alpha\beta} \hat{n}_{i\alpha\uparrow} \hat{n}_{i\beta\downarrow} \quad (1)$$

Here α, β are orbital indices, i, j run over the atomic positions within the unit cell and l, l' refer to lattice vectors. U , the strength of the on-site Hubbard interaction, is assumed to be site and orbital independent.

We solve the many-body problem by Cluster Perturbation Theory (CPT).²⁴ CPT has been successfully used to

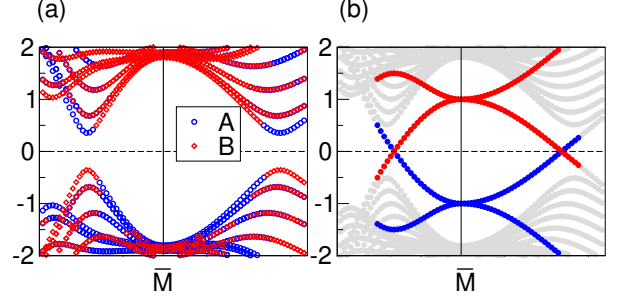


FIG. 3. a) Single-particle Projected Bulk Band Structure calculated along high-symmetry directions of the 2D Brillouine Zone of Fig. 1 (c) around \bar{M} point. In blue (red) eigenvalues with predominant A- (B) character. (b) Eigenvalues obtained for a slab of 20 A-B bilayers. In blue (red) eigenstates localized at the lower (upper) surface layer containing A (B) sites.

study Mott-Hubbard physics both in model systems^{24,35} and in real materials,^{36–38} and more recently to address correlated topological phases of matter.^{21–23,39}

CPT belongs to the class of Quantum Cluster theories which solve the problem of many interacting electrons in an extended lattice by approaching first the many body problem in a subsystem of finite size - a cluster- and then embedding it within the infinite medium.⁴⁰ The lattice is seen as a periodic repetition of identical clusters each of them containing M atoms characterized by a set of n_i^{orb} orbitals ($K = \sum_i^M n_i^{orb}$ is the total number of sites/orbitals per cluster). The Hamiltonian is then partitioned in two terms, an intra-cluster and an inter-cluster one. Since the e-e Coulomb interaction is on-site, the inter-cluster Hamiltonian contains only single particle hopping terms and the many body part is present in the intra-cluster Hamiltonian only. The Green's function for the extended lattice can then be obtained by solving the equation

$$G_{ij\alpha\beta}(k, \omega) = G_{i\alpha j\beta}^c(\omega) + \sum_{i'\delta} B_{i\alpha i'\delta}(k, \omega) G_{i'\delta j\beta}(k, \omega). \quad (2)$$

Here the $K \times K$ matrix $B_{i\alpha i'\delta}(k, \omega)$ is given by

$$B_{i\alpha i'\delta}(k, \omega) = \sum_l^L e^{ik \cdot R_l} \sum_{i''}^M \sum_{\gamma} G_{i\alpha i''\gamma}^c(\omega) t_{i''\gamma 0, i'\delta l}$$

with R_l the lattice vectors and $t_{i''\gamma 0, i'\delta l}$ the hopping between site i' and i'' belonging to different clusters. $G_{i\alpha j\beta}^c$ is the Green's function obtained by exact diagonalization of the interacting Hamiltonian for the finite cluster; we separately solve the problem for N , $N-1$ and $N+1$ electrons and express the cluster Green's function in the Lehmann representation at real frequencies.⁴¹

For the tetragonal lattice, the 4-site cluster shown in Fig. 1 (a) has been adopted. This choice is suggested by

the strength of hopping parameters: in the present model the largest hopping parameters are those connecting A-B sites. They are included in the exact diagonalization while the smaller ones are used, in the spirit of CPT, *perturbatively* in the periodization of the cluster Green's function.

Once the cluster Green's function in the local basis $G_{i\alpha i'\beta}^c(\omega)$ has been calculated by exact diagonalization, eq. 2 is solved by matrix inversion at each k and ω . The quasi-particle band structure is then obtained in terms of spectral function $A(k\omega)$

$$A(k\omega) = \frac{1}{\pi} \sum_n \text{Im} G(kn\omega). \quad (3)$$

where

$$G(kn\omega) = \frac{1}{K} \sum_{ii'} e^{-ik \cdot (r_i - r_{i'})} C_{i\alpha}^n(k) G_{ii'}(k, \omega)$$

Here n is the band index and $C_{i\alpha}^n(\mathbf{k})$ are the eigenstate coefficients obtained by the single-particle band calculation.³⁶

Results. We compare now the spectral function obtained for the bulk crystal with increasing values of U . We see that the minimum energy separation between hole and particle excitations - the quasi-particle gap Δ - diminishes with U and goes to zero at a critical value $U_c = 2.5$. After that, Δ keeps increasing linearly as in a standard Mott-Hubbard regime. This behaviour resembles quite closely what happens in the Kane-Mele-Hubbard model which describes graphene as a Quantum Spin Hall topological insulator in the presence of on-site e-e interaction^{21-23,42}.

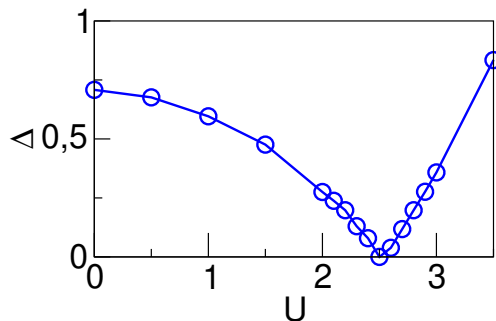


FIG. 4. Evolution of the minimum energy separation between hole and particle excitations as a function of the strength of the U -parameter

Fig 5 shows the quasiparticle band structure of bulk CTI for different values of U around the critical value U_c . In order to elucidate the orbital composition of the quasi-particle states we plot the *local* spectral function $A(k\omega) = \frac{1}{\pi} \sum_n \text{Im} G(kn\omega) |C_{i\alpha}^n(k)|^2$ with α running over

the two orbitals of site A (right panel) or B (left panel). We see that for $U < U_c$ states close to the Fermi level have a predominant A -site or B -site character.

For $U \geq U_c$ this is no more the case and the states that are close to the Fermi level exhibit a mixed A - B composition. The orbital texture in the bulk evolves then with U : below U_c valence and conduction band edges exhibit the same band inversion that has been identified in the non-interacting system with the predominant contribution from A and B sites alternating around the A point (or the \bar{M} point in the PBBS). This band inversion fades away for $U \geq U_c$ where states close to the Fermi level have a mixed A - B character.

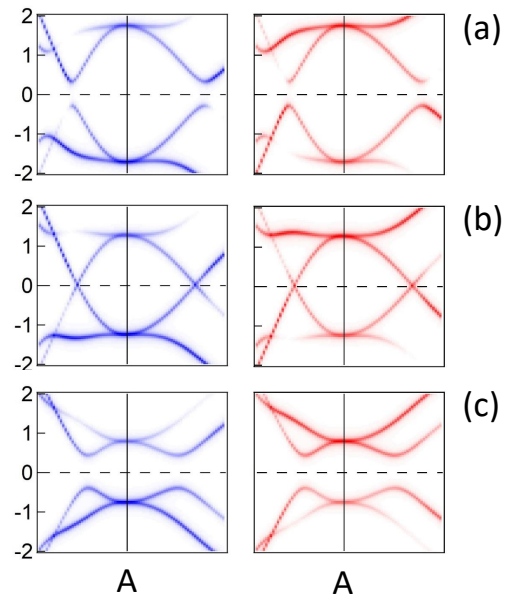


FIG. 5. Site selected bulk quasi-particle states at k -points where the minimum energy separation between hole and particle states occurs. Panels (a), (b), (c) correspond to $U = 1, 2.5, 3.5$ respectively. The left (right) panels in blue (red) show the A -site (B -site) contribution.

Simultaneously, as band inversion disappears, surface states lose their metallic character and a gap appears in their k -dispersion. This is shown in Fig. 6 where the local spectral functions obtained for the 20-layer slab are shown for the same U values. In the non interacting CTI the existence of gapless surface states has been associated to a topological phase; we see that this phase persists only up to $U < U_c$.

In conclusion, we have demonstrated that the Hubbard interaction modifies the orbital texture of the quasi-particle band edges around the Fermi level; this effect is remarkable and can be relevant also in real materials exhibiting CTI behaviour. Above the critical value U_c band inversion is removed and surface states are gapped. This suggests the identification of this critical value as a transi-

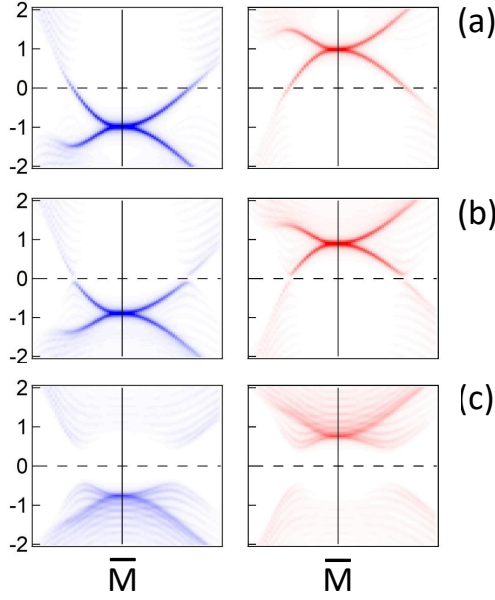


FIG. 6. Surface quasi-particle states for increasing U across U_c . Panels (a), (b), (c) correspond to $U = 1, 2.5, 3.5$ respectively. The left (right) panels in blu (red) show states localized at the A -site (B -site) terminated surface.

tion point from a topological to a trivial insulating phase. An explicit confirmation of topological character and of its evolution with U would require the generalization to the interacting case of the new Z_2 topological invariant that has been introduced to classify the topological crystalline insulator phase in the non interacting system.¹ The so-called *topological Hamiltonian*^{43,44} - a fictitious non-interacting Hamiltonian associated to the inverse of the dressed Green's function at zero frequency - would be the most promising approach. It has been applied to identify the topological character of heavy fermion mixed valence compounds⁴⁵⁻⁴⁸ and of the half-filled honeycomb lattice^{22,23} in the presence of on-site Hubbard interaction. The application of this method to CTIs will be the subject of a forthcoming paper.

¹ L. Fu, Phys. Rev. Lett. **106**, 106802 (2011).

² T. H. Hsieh, H. Lin, J. Liu, W. Duan, A. Bansil, and L. Fu, Nature Communications **3**, 982 (2012).

³ Y. Tanaka, Z. Ren, T. Sato, K. Nakayama, S. Souma, T. Takahashi, K. Segawa, and Y. Ando, Nature Physics **8**, 800 (2012).

⁴ P. Dziawa, B. J. Kowalski, K. Dybko, R. Buczko, A. Szczerbakow, M. Szot, E. Łusakowska, T. Balasubramanian, B. M. Wojek, M. H. Berntsen, O. Tjernberg, and T. Story, Nature Materials **11**, 1023 (2012).

⁵ S.-Y. Xu, C. Liu, N. Alidoust, M. Neupane, D. Qian, I. Belopolski, J. D. Denlinger, Y. J. Wang, H. Lin, L. A. Wray, G. Landolt, B. Slomski, J. H. Dil, A. Marcinkova, E. Morosan, Q. Gibson, R. Sankar, F. C. Chou, R. J. Cava, A. Bansil, and M. Z. Hasan, Nature Communications **3**, 1192 (2012).

⁶ Y. J. Wang, W.-F. Tsai, H. Lin, S.-Y. Xu, M. Neupane, M. Z. Hasan, and A. Bansil, Phys. Rev. B **87**, 235317 (2013).

⁷ Y. Okada, M. Serbyn, H. Lin, D. Walkup, W. Zhou, C. Dhital, M. Neupane, S. Xu, Y. J. Wang, R. Sankar, F. Chou, A. Bansil, M. Z. Hasan, S. D. Wilson, L. Fu, and V. Madhavan, Science **341**, 1496 (2013), <https://science.sciencemag.org/content/341/6153/1496.full.pdf>.

⁸ I. Zeljkovic, Y. Okada, C.-Y. Huang, R. Sankar, D. Walkup, W. Zhou, M. Serbyn, F. Chou, W.-F. Tsai, H. Lin, A. Bansil, L. Fu, M. Z. Hasan, and V. Madhavan, Nature Physics **10**, 572 (2014).

⁹ Y. Ando and L. Fu, Annual Review of Condensed Matter Physics **6**, 361 (2015), <https://doi.org/10.1146/annurev->

[conmatphys-031214-014501](https://doi.org/10.1146/annurev-conmatphys-031214-014501).

¹⁰ T. H. Hsieh, J. Liu, and L. Fu, Phys. Rev. B **90**, 081112 (2014).

¹¹ H. Weng, J. Zhao, Z. Wang, Z. Fang, and X. Dai, Phys. Rev. Lett. **112**, 016403 (2014).

¹² H. Isobe and L. Fu, Phys. Rev. B **92**, 081304 (2015).

¹³ M. Kargarian and G. A. Fiete, Phys. Rev. Lett. **110**, 156403 (2013).

¹⁴ M. Hohenadler and F. F. Assaad, Journal of Physics: Condensed Matter **25**, 143201 (2013).

¹⁵ Z. Y. Meng, H.-H. HUNG, and T. C. LANG, Modern Physics Letters B **28**, 1430001 (2014).

¹⁶ S. Rachel, Reports on Progress in Physics **81**, 116501 (2018).

¹⁷ S. Rachel and K. Le Hur, Phys. Rev. B **82**, 075106 (2010).

¹⁸ D. Zheng, G.-M. Zhang, and C. Wu, Phys. Rev. B **84**, 205121 (2011).

¹⁹ M. Hohenadler, T. C. Lang, and F. F. Assaad, Phys. Rev. Lett. **106**, 100403 (2011).

²⁰ M. Hohenadler, Z. Y. Meng, T. C. Lang, S. Wessel, A. Muramatsu, and F. F. Assaad, Phys. Rev. B **85**, 115132 (2012).

²¹ S.-L. Yu, X. C. Xie, and J.-X. Li, Phys. Rev. Lett. **107**, 010401 (2011).

²² F. Grandi, F. Manghi, O. Corradini, C. M. Bertoni, and A. Bonini, New Journal of Physics **17**, 023004 (2015).

²³ .

²⁴ D. Sénéchal, D. Perez, and M. Pioro-Ladrière, Phys. Rev. Lett. **84**, 522 (2000).

²⁵ D. Sénéchal, "Cluster perturbation theory," in *Theoretical*

- methods for Strongly Correlated Systems*, Springer Series in Solid-State Sciences, Vol. 171 (Springer, 2012) Chap. 8, pp. 237–269.
- ²⁶ J. Liu, T. H. Hsieh, P. Wei, W. Duan, J. Moodera, and L. Fu, *Nature Materials* **13**, 178 (2014).
 - ²⁷ C.-Y. Huang, H. Lin, Y. J. Wang, A. Bansil, and W.-F. Tsai, *Phys. Rev. B* **93**, 205304 (2016).
 - ²⁸ D. Walkup, B. A. Assaf, K. L. Scipioni, R. Sankar, F. Chou, G. Chang, H. Lin, I. Zeljkovic, and V. Madhavan, *Nature Communications* **9**, 1550 (2018).
 - ²⁹ B. M. Wojek, P. Dziawa, B. J. Kowalski, A. Szczerbakow, A. M. Black-Schaffer, M. H. Berntsen, T. Balasubramanian, T. Story, and O. Tjernberg, *Phys. Rev. B* **90**, 161202 (2014).
 - ³⁰ H. Zhang, C.-X. Liu, and S.-C. Zhang, *Phys. Rev. Lett.* **111**, 066801 (2013).
 - ³¹ Y. Cao, J. A. Waugh, X.-W. Zhang, J.-W. Luo, Q. Wang, T. J. Reber, S. K. Mo, Z. Xu, A. Yang, J. Schneeloch, G. D. Gu, M. Brahlek, N. Bansal, S. Oh, A. Zunger, and D. S. Dessau, *Nature Physics* **9**, 499 (2013).
 - ³² B. A. Bernevig, T. L. Hughes, and S.-C. Zhang, *Science* **314**, 1757 (2006), <https://science.sciencemag.org/content/314/5806/1757.full.pdf>.
 - ³³ C. Liu, T. L. Hughes, X.-L. Qi, K. Wang, and S.-C. Zhang, *Phys. Rev. Lett.* **100**, 236601 (2008).
 - ³⁴ F. Manghi, C. Calandra, and E. Molinari, *Surface Science* **184**, 449 (1987).
 - ³⁵ M. Potthoff, M. Aichhorn, and C. Dahnken, *Phys. Rev. Lett.* **91**, 206402 (2003).
 - ³⁶ F. Manghi, *Journal of Physics: Condensed Matter* **26**, 015602 (2014).
 - ³⁷ R. Eder, *Phys. Rev. B* **78**, 115111 (2008).
 - ³⁸ R. Eder, *Phys. Rev. B* **91**, 245146 (2015).
 - ³⁹ M. Puviani and F. Manghi, *Phys. Rev. B* **94**, 161111 (2016).
 - ⁴⁰ T. Maier, M. Jarrell, T. Pruschke, and M. H. Hettler, *Rev. Mod. Phys.* **77**, 1027 (2005).
 - ⁴¹ More details on CPT implementation for multi-orbital systems can be found in <https://www.cond-mat.de/events/correl16/manuscripts/manghi.pdf>.
 - ⁴² W. Wu, S. Rachel, W.-M. Liu, and K. Le Hur, *Phys. Rev. B* **85**, 205102 (2012).
 - ⁴³ Z. Wang, X.-L. Qi, and S.-C. Zhang, *Phys. Rev. B* **85**, 165126 (2012).
 - ⁴⁴ Z. Wang and S.-C. Zhang, *Phys. Rev. X* **2**, 031008 (2012).
 - ⁴⁵ J. Werner and F. F. Assaad, *Phys. Rev. B* **88**, 035113 (2013).
 - ⁴⁶ X. Deng, K. Haule, and G. Kotliar, *Phys. Rev. Lett.* **111**, 176404 (2013).
 - ⁴⁷ F. Lu, J. Zhao, H. Weng, Z. Fang, and X. Dai, *Phys. Rev. Lett.* **110**, 096401 (2013).
 - ⁴⁸ T. Yoshida, R. Peters, S. Fujimoto, and N. Kawakami, *Phys. Rev. B* **87**, 085134 (2013).